

Investigating the spatial distribution of resident's outdoor heat exposure across neighborhoods of Philadelphia, Pennsylvania using urban microclimate modeling

Xiaojiang Li

Department of Geography and Urban Studies, Temple University, Philadelphia, PA, United States



ARTICLE INFO

Keywords:

Thermal comfort
Mean radiant temperature
Urban thermal inequity
GIS
SOLWEIG

ABSTRACT

Cities are experiencing more and more frequent extreme heat events in hot summers in the context of rising global temperatures. A precise understanding of the spatial distribution of the human outdoor heat exposure across neighborhoods in cities is of great importance for urban heat management. Different from remote sensing based the land surface temperature, this study calculated the mean radiant temperature, which is more objective to indicate human heat stress, to study the spatial distribution of human outdoor heat exposure in Philadelphia, Pennsylvania. The SOLWEIG (SOlar and LongWave Environmental Irradiance Geometry) model was applied to estimate the mean radiant temperature based on the high-resolution urban 3D model and meteorological data. This study further examined the spatial distributions of heat exposure levels across neighborhoods of different groups in Philadelphia. Results show that there is no significant disparity in terms of outdoor heat exposure levels for different racial/ethnic groups in Philadelphia. Generally, the elderly, who usually are more vulnerable to extreme heat, tend to live in neighborhoods with less outdoor heat exposure in summer ($p < 0.001$). The higher-income people tend to live in thermally more comfortable neighborhoods ($p < 0.001$). The study provides a precise understanding of the heat distribution across neighborhoods, which would further help to develop strategies to allocate resources to the most needed neighborhoods to maximumly mitigate the negative impact of urban heat.

1. Introduction

The increasingly frequent and intense extreme heat events in large U.S. cities cause more climate-related mortalities than any other hazardous weather event (Borden & Cutter, 2008; Stone, Hess, & Frumkin, 2010). In the context of global warming, heat waves are supposed to be more frequent and intense in many cities (Alexander & Arblaster, 2009). In addition, the urban heat island effect is believed to further exacerbate the mortality increase caused by heat stress in cities (Gabriel & Endlicher, 2011). The summer heatwaves would also increase the deaths and illnesses caused by infectious disease and air pollution (Easterling et al., 2000; McPhearson, Mustafa, & Ortiz, 2020; Patz, Campbell-Lendrum, Holloway, & Foley, 2005). Therefore, studying the extreme urban heat and its impacts on urban residents is of great importance for building thermally comfortable and climate-resilient cities.

The extreme urban heat is not distributed evenly across neighborhoods of cities, and not all populations are impacted by the extreme heat

equally (Hsu, Sheriff, Chakraborty, & Manya, 2021; McDonald et al., 2021; Reid et al., 2009). Hsu et al. (2021) investigated the heat exposure distribution using land surface temperature and found that the people of color tend to have more exposure to urban heat island exposure in major US cities. McDonald et al. (2021) found that low-income neighborhoods are 1.5 °C hotter than high-income neighborhoods in 93 municipalities of US. Those neighborhoods with more green spaces tend to be less vulnerable to the summertime extreme heat since the urban green space can mitigate the urban heat island effect and the tree canopies help to provide shade (Arnberger et al., 2017; Doick, Peace, & Hutchings, 2014; Kong, Yin, James, Hutyra, & He, 2014). The marginalized groups (low-income people, minorities) are generally more vulnerable to summer heat waves (CDC, Center for Disease Control, 2004; Reid et al., 2012) for different socio-economic reasons. The elderly and young children are usually more vulnerable to extreme heat than those physically healthy young adults (McGeehin & Mirabelli, 2001; Medina-Ramón, Zanobetti, Cavanagh, & Schwartz, 2006). Those people with preexisting health conditions are more vulnerable to extreme heat

E-mail address: lixiaojiang.gis@gmail.com.

(McGeehin & Mirabelli, 2001; Schwartz, 2005). In addition, the accessibility to air-conditioning also impact people's vulnerability to summer extreme heat.

A fine level of quantitative information about where and which populations are vulnerable to heat is important to identify the most vulnerable neighborhoods and populations in order to mitigate the negative impacts of heat on urban residents (Gronlund, 2014; Reid et al., 2012). The ground surface temperature estimated from remotely sensed thermal imageries has been widely used to map the intensity of the heat at large scales (Chen, Zhao, Li, & Yin, 2006; Equeure, Mirzaei, & Riffat, 2020; Guo et al., 2020; Johnson, Stanforth, Lulla, & Luber, 2012; Shandas, Voelkel, Williams, & Hoffman, 2019; Yang et al., 2019). The overhead view remote sensing can cover a broad spatial extent rapidly and periodically, which makes it an efficient tool to investigate the spatio-temporal distributions of ground surface temperature. However, the land surface temperature derived from remotely sensed imageries cannot fully represent human actual outdoor heat exposure. This is because human heat exposure is also impacted by other factors, such as shade, wind speed, humidity (Klemm, Heusinkveld, Lenzholzer, & van Hove, 2015; Norton et al., 2015), while those factors are usually not covered in the remotely sensed imageries, which usually indicate the surface temperature of the ground, building roofs, and the top of tree canopies. Although the remotely sensed imagery can estimate the land surface temperature of a large geographical area rapidly, however, it is still not able to detect the temporal variations of the heat exposure on a daily level. In addition, the remote sensing-derived land surface temperature usually cannot show the fine-level spatial variations of human outdoor heat exposure across neighborhoods because of the relatively coarse resolution of the thermal imageries.

The urban microclimate modeling based on high resolution 3D urban models and meteorological data makes it possible to examine how people are exposed to heat stress at a fine spatio-temporal level (Huang, Cedeno-Laurent, & Spengler, 2014; Lindberg & Grimmond, 2011; Lindberg & Grimmond, 2011; Matzarakis, Rutz, & Mayer, 2010). By simulating how the solar radiation reaching the ground, it is possible to compute the mean radiant temperature (T_{mrt}), which is the total net short and long-wave radiation a human exposed to the surrounding environment and has the strongest influence on human energy balance (Ali-Toudert & Mayer, 2007; Matzarakis et al., 2010; Mayer & Höpke, 1987; Thorsson et al., 2014). The urban microclimate modeling also makes it possible to examine the impacts of urban canyons and urban landscapes on the human heat exposure, which would benefit urban design practices for urban heat management (Fröhlich, Gangwisch, & Matzarakis, 2019; Rodríguez-Algeciras, Tablada, Chaos-Yeras, De la Paz, & Matzarakis, 2018). Therefore, this study applied urban microclimate modeling to calculate and map the spatial distribution of the T_{mrt} across neighborhoods in Philadelphia to indicate human outdoor heat exposure. The high-resolution 3D urban model generated from LiDAR and land use map together with the meteorological data were used as the input to represent the urban geometry and local climate context for modeling human outdoor heat exposure, respectively. In order to examine the potential inequities in terms of outdoor heat exposure among different neighborhoods and population groups, this study further compared the T_{mrt} with the socio-economic statuses of residents in different neighborhoods.

2. Methodology

2.1. Study area and data sources

The local climate in Philadelphia is humid subtropical, which features hot and humid summers. In order to indicate the local climate, this study collected the meteorological data that includes the air temperature, direct radiation, diffuse radiation, humidity, and wind speed from the NREL (<https://www.nrel.gov/research/data-tools.html>). The meteorological data of 2018 from June 1st to August 31st at an hourly level

was used in this study. In order to generate the urban 3D models, this study first created the normalized digital surface model (nDSM) based on the LiDAR cloud points using ArcGIS (Fig. 1(b)). The building height model and tree canopy height model were then created by overlaying the most recent land cover map (Fig. 1(a)) on the generated nDSM. The high-resolution LiDAR cloud point and the land cover map with a spatial resolution of 1 m were accessed from the Pennsylvania Spatial Data Access Portal (<https://www.pasda.psu.edu/>).

2.2. Human outdoor heat exposure estimation

As one of the most important factors that influence human energy balance and thermal comfort (Ali-Toudert & Mayer, 2007; Matzarakis et al., 2010; Mayer & Höpke, 1987; Thorsson et al., 2014), the mean radiant temperature (T_{mrt}) was used to indicate human heat exposure in this study. There are several existing widely used tools to compute the T_{mrt} , like ENVI-met (Bruse, 2004; Huttner, 2012), RayMan (Matzarakis, Rutz, & Mayer, 2007, 2010), and SOLWEIG (SOLar and LongWave Environmental Irradiance Geometry) model (Lindberg, Holmer, & Thorsson, 2008, 2018). In order to generate a large scale T_{mrt} map, this study customized the open-sourced SOLWEIG model for computing the continuous distribution of T_{mrt} in Philadelphia. The SOLWEIG has been applied and validated worldwide (Chen, Yu, Yang, & Mayer, 2016; Gál & Kántor, 2020; Lindberg & Grimmond, 2011; Lindberg, Onomura, & Grimmond, 2016; Thorsson, Lindberg, Björklund, Holmer, & Rayner, 2011). Similar to the climate zone of the study area, the SOLWEIG model has also been validated in the humid sub-tropical climate, and modeling results show a well match with the measurements (Chen et al., 2016; Lau, Ren, Ho, & Ng, 2016). Therefore, the SOLWEIG model was used to calculate the T_{mrt} in this study based on the high-resolution building height model, tree canopy height model, together with meteorological data (Fig. 2).

In order to better represent the human outdoor heat exposure level in the summer, this study calculated the T_{mrt} at hour level from 11 a.m. to 2 p.m. every day from June 1st to August 31st in 2018, since these are considered the hottest times of one year and the most recent available meteorological data is in 2018. By aggregating the calculated hour-level T_{mrt} , this study then calculated the mean T_{mrt} to indicate the overall outdoor heat exposure level in the summer. Since the SOLWEIG model is too time consuming for city-scale T_{mrt} estimation, therefore, the input high resolution urban 3D models were chopped into small tiles. To solve the bias on the edges of tiles due to abrupt change on borders caused by splitting, a buffer zone of 150 m was added to each tile. This study further run the SOLWEIG model on high performance computer to estimate the T_{mrt} for those tiles, which were then mosaiced to cover the whole study area. Those buffered zones were removed in mosaicking to generate the T_{mrt} map for the whole study area.

2.3. Environmental injustice analyses

Previous studies have reported the thermal inequities in US cities and found that lower socioeconomic groups and minorities are generally exposed to a higher level of urban heat risk (Harlan, Brazel, Prashad, Stefanov, & Larsen, 2006; Mitchell & Chakraborty, 2015, 2018). This study examined the urban heat exposure among different groups of people in Philadelphia at a finer level using urban microclimate modeling. In order to examine the different T_{mrt} distributions among different neighborhoods of Philadelphia, this study conducted statistical analyses to investigate the associations between the T_{mrt} and explanatory variables that represent resident's race/ethnicity and socio-economic status. Those explanatory variables were selected based on previous studies on environmental inequities (Huang, Zhou, & Cadenasso, 2011; Kim & Chun, 2019; Landry & Chakraborty, 2009; Lin, Wang, & Li, 2021; Mitchell & Chakraborty, 2018; Li, Zhang, Li, & Kuzovkina, 2016). To represent the race and ethnicity of residents in different neighborhoods, this study calculated variables of the

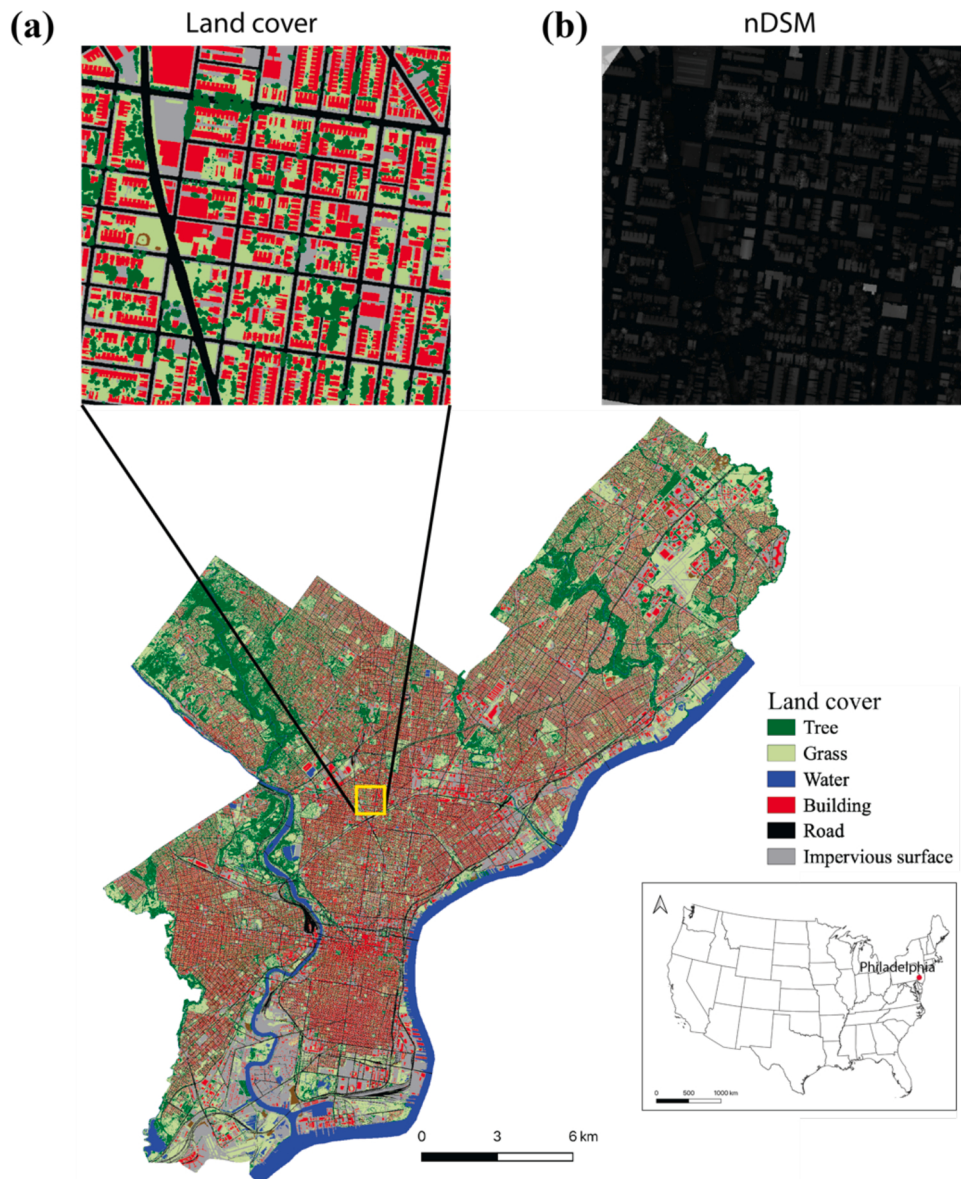


Fig. 1. The location and datasets of the study area, (a) a patch of the land cover map in the study area, (b) the normalized digital surface model (nDSM) of a portion of the study area.

proportion of non-Hispanics Whites, the proportion of African Americans, the proportion of Hispanics, and the proportion of Asian Americans based on the American Community Survey census data (ACS 2014–2018 5-year data). To represent the socio-economic status, this study further derived variables of per capita income, the proportion of people older than 65, the proportion of people younger than 18, the proportion of people with bachelor or higher degrees, and the proportion of people without high-school degrees from ACS 2014–2018 5-year data. To make the pixel-level T_{mrt} comparable to the census data, the pixel-level T_{mrt} were aggregated at the census tract level using mean value. Since the calculated T_{mrt} focuses on pedestrian radiation fluxes (Lindberg & Grimmond, 2011), therefore, the T_{mrt} pixels for building roofs and water bodies were masked out while aggregating the pixel-level T_{mrt} to the census tract level.

The ordinary least square (OLS) multivariate regression model was applied to investigate the associations between the explanatory variables and the T_{mrt} at the census tract level. Only those explanatory variables that are significantly correlated with the T_{mrt} ($p < 0.05$) were selected as independent variables in the regression analysis. The global

Moran's I statistic was used to determine whether the regression results were spatially biased because of spatial autocorrelation. The spatial regression model with consideration of the spatial dependence was then applied if a significant spatial autocorrelation was detected among the OLS regression model.

3. Results

3.1. Spatial distribution of the T_{mrt}

Fig. 3 shows the spatial distribution of the average T_{mrt} in Philadelphia in the summer of 2018. Generally, the distribution of the T_{mrt} matches very well with the tree canopy cover and those areas with more tree canopies tend to have lower T_{mrt} (**Fig. 3a**). This is because the tree canopies would provide shade and help to reduce heat exposure on the ground. The northwestern and the northeastern parts of the study area have significantly lower T_{mrt} than the eastern and southern parts. Those eastern and southern parts that feature dense low-rise building blocks and low tree canopy covers have high T_{mrt} (**Fig. 3b**). Although with a

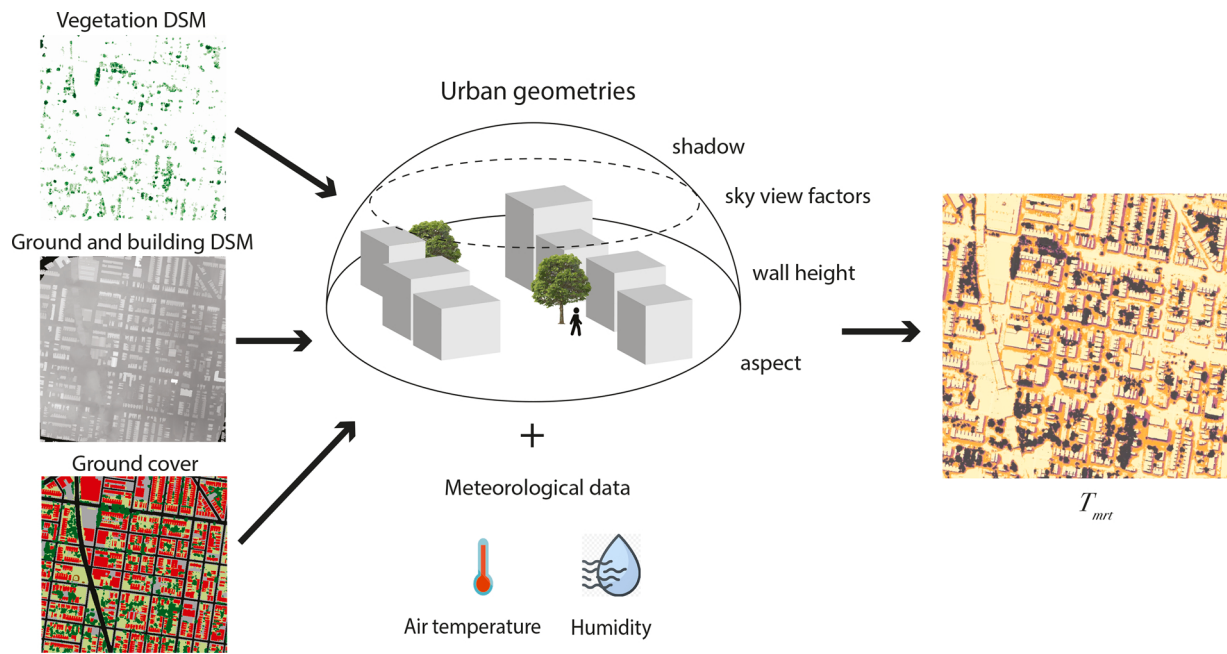


Fig. 2. The calculation of mean radiant temperature (T_{mrt}) using the SOLWEIG model based on tree canopy height model, ground and building height model, land cover, and meteorological data.

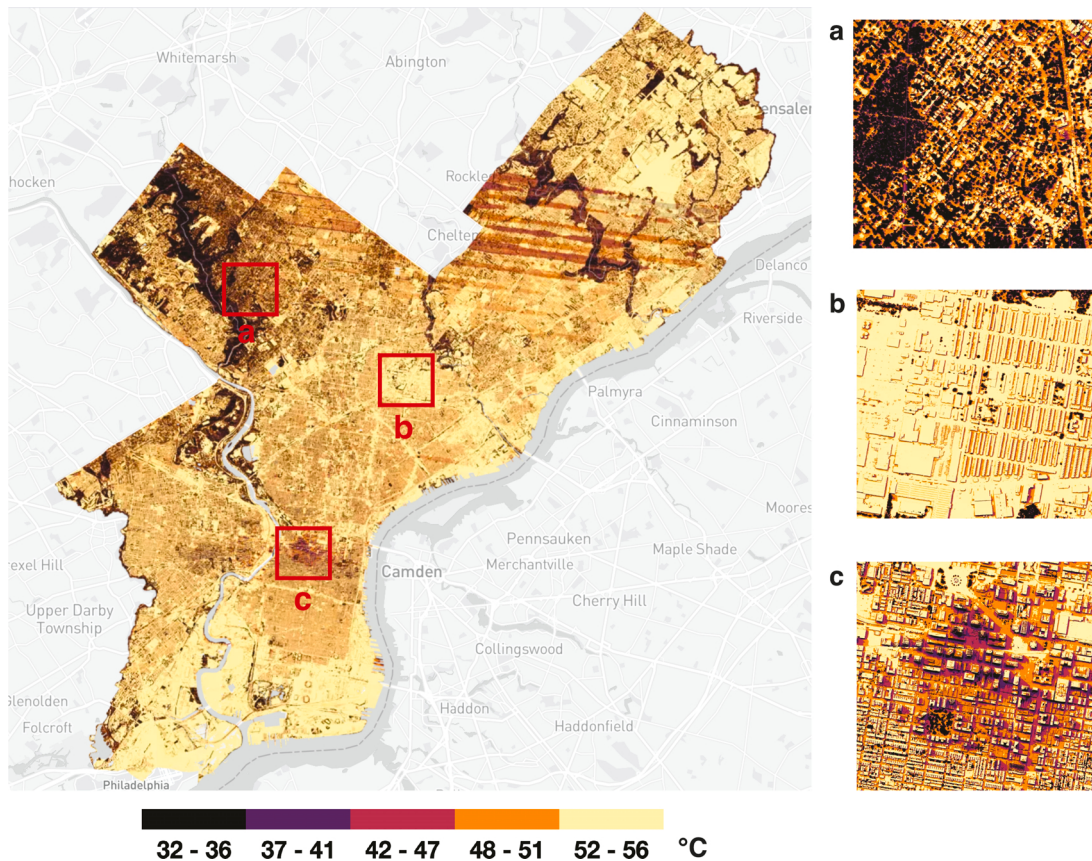


Fig. 3. The spatial distribution of the average T_{mrt} in the study area and three typical regions from June 1st - August 31, 2018, (a) a region with large tree canopy cover and low T_{mrt} , (b) a typical region features concrete checkboard building blocks and high T_{mrt} , (c) a typical region in the downtown area with high-rise buildings and relatively low T_{mrt} .

relatively low tree canopy cover, the downtown area of Philadelphia (the region Fig. 3c) has relatively low T_{mrt} . The low outdoor heat exposure in the downtown area can be explained by the shade provision

of high-rise building blocks there. Please note that the T_{mrt} map has some stripes in the northeastern part, which are caused by noise in the raw LiDAR cloud point.

Fig. 4 shows the aggregated T_{mrt} at the census tract level based on the pixel level T_{mrt} by masking out water and building roof pixels. Generally, those census tracts in the eastern and the southern parts have higher T_{mrt} . Those census tracts in the northwestern and northeastern parts have relatively low T_{mrt} . This is because of the large canopy cover in the northwestern and northeastern regions, and the tree canopies help to block the solar radiation and lower the T_{mrt} significantly. In addition, the downtown area also has relatively low T_{mrt} , which can be explained by the shadow casted by high-rise buildings.

3.2. Socio-environmental analysis results

Fig. 5 shows the scatter plots and the correlation coefficients of the census tract level T_{mrt} and different urban form variables, the percentage of tree canopy cover, the average tree canopy height, the percentage of the impervious surface, and the average building height. The percentage of tree canopy cover (**Fig. 4(a)**), the average tree canopy height (**Fig. 4(b)**), and the average building height (**Fig. 4(d)**) have a significant and negative correlation with the T_{mrt} at the census tract level, while the percentage of the impervious surface is significantly and positively correlated with the T_{mrt} (**Fig. 4(c)**). These correlations indicate that the tree canopy cover and the average height of building and tree canopies would help to reduce the potential outdoor heat exposure in hot summer, while the percentage of the impervious surface would increase the

human outdoor heat exposure.

Table 1 shows the correlation coefficients between the T_{mrt} and the selected explanatory variables at the census tract level. The per capita income has a significant and negative correlation with the T_{mrt} , which indicates that the rich people tend live in neighborhoods with low outdoor heat exposure. The proportion of people without high school degrees is significantly and positively correlated with the T_{mrt} , while the proportion of people with the bachelor or higher degrees is significantly and negatively correlated with the T_{mrt} . The proportion of non-Hispanic Whites has a significant and negative correlation with the T_{mrt} , however, the proportion of Hispanics has a significant and positive correlation with the T_{mrt} . The proportion of African Americans and the proportion of Asian Americans are both not significantly correlated with the T_{mrt} . The proportion of people under 18 years of age is significantly and positively correlated with the T_{mrt} , while the proportion of people older than 65 years of age is significantly and negatively correlated with the T_{mrt} .

Based on the correlation analysis results, the per capita income, the proportion of Hispanics, the proportion of people under 18 years of age, and the proportion of people older than 65 years of age were used in the regression model. The educational variables were identified as the confounded variables of the per capita income, and were excluded from the regression analysis. **Table 2** presents the results of OLS regression model at the census tract level. The OLS multivariate regression model helps to explain 30 % of the variation in the T_{mrt} change for the 376

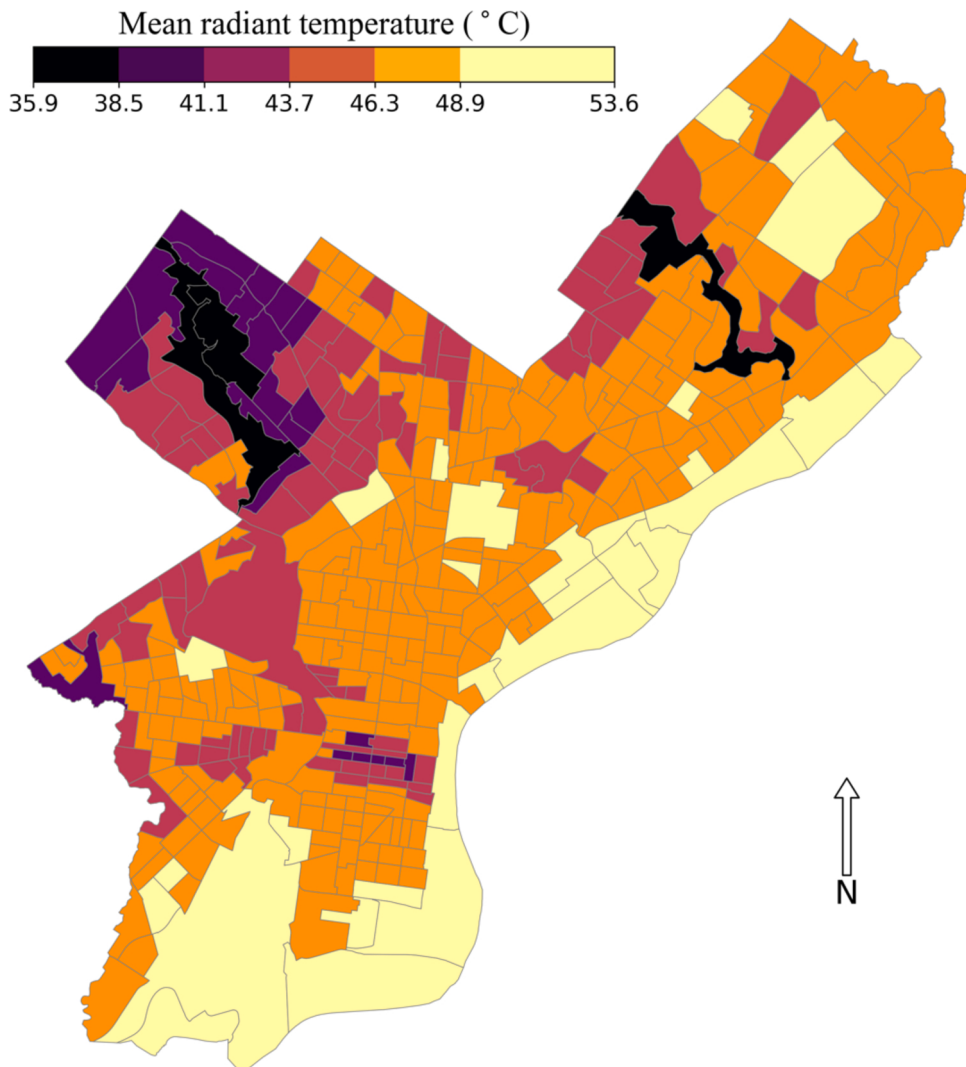


Fig. 4. The spatial distribution of the aggregated mean radiant temperature (T_{mrt}) at the census tract level in the study area.

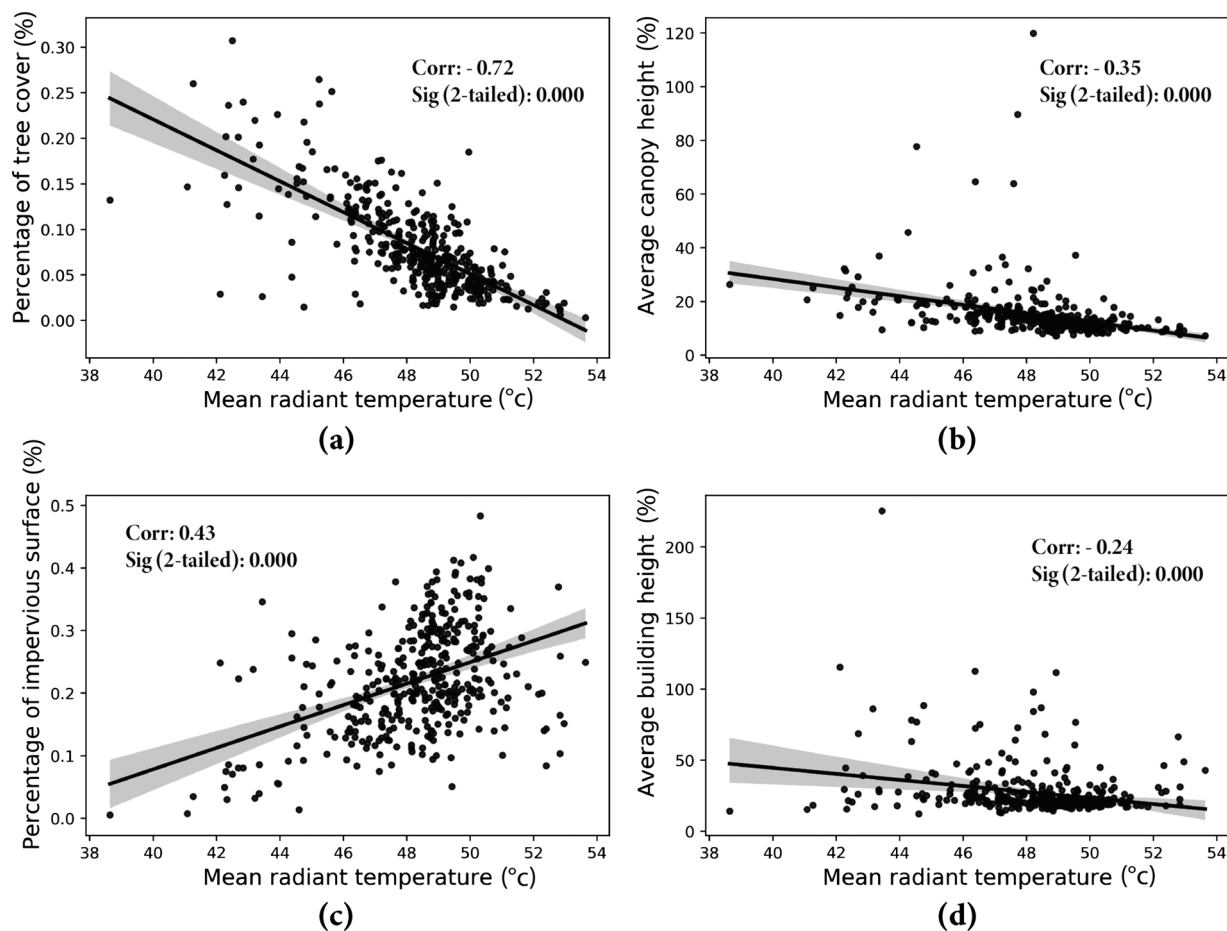


Fig. 5. The scatter plots and correlations between the T_{mrt} and the urban form variables at the census tract level ($N = 376$), (a) the percentage of tree canopy cover and the T_{mrt} , (b) the average tree canopy height (feet) and the T_{mrt} , (c) the percentage of impervious surface and the T_{mrt} , (d) the average building height (feet) and the T_{mrt} .

Table 1

The correlations coefficients between the T_{mrt} and the selected socio-economic variables.

Category	Variables	Pearson's correlation	Sig (2-tailed)	N
Economic status	Per capita income	-0.49**	0.000	
Education	Proportion of people without high school degree	0.49**	0.000	
	Proportion of people with bachelor or higher degrees	-0.44**	0.000	
	Proportion of non-Hispanic Whites	-0.26**	0.000	
Race and ethnicity	Proportion of Hispanics	0.31**	0.000	376
	Proportion of African Americans	0.09	0.071	
	Proportion of Asian Americans	0.04	0.446	
	Proportion of people under 18 years of age	0.35**	0.000	
Age	Proportion of people older than 65 years of age	-0.39**	0.000	

** Correlation is significant at the 0.01 level (2-tailed).

census tracts of the study area. The per capita income and the proportion of people older than 65 years of age are significantly and negatively associated with the T_{mrt} , which means that those census tracts with higher per capita income or larger proportion of people older than 65

Table 2

Ordinary least squares (OLS) regression model and spatial lag model (SAR_{lag}) of mean radiant temperature (T_{mrt}) and independent variables at census tract level in the study area.

Variables	OLS Coefficients (z-values)	SAR _{lag} Coefficients (z-values)
Constant	50.0862 **	15.46 **
Per capita income (thousand dollar)	-0.04 (-6.95 **)	-0.02 (-4.10 **)
Proportion of Hispanics	1.30 (2.21 *)	0.14 (0.33)
Proportion of people under 18 years of age	0.36 (0.26)	-0.85 (-0.86)
Proportion of people older than 65 years of age	-6.27 (-4.78 **)	-3.45 (-3.67 **)
R ²	0.31	
Rho		0.70
Adjusted R ²	0.30	
F-statistic	41.85 **	
Akaike info criterion		1268.98
Moran's I of residuals	0.51 (16.98 **)	

* Significant at the 0.05 level (2-tailed).

** Significant at the 0.01 level (2-tailed).

years old age have lower outdoor heat exposure during summer. The proportion of Hispanics has a weakly and positively significant association with the T_{mrt} . The proportion of people under 18 years of age has no significant association with the T_{mrt} in the study area.

The spatial dependence of the residuals in the OLS model shows a significant spatial autocorrelation (Moran's $I = 0.51$, z score = 16.98), therefore, this study further applied the spatial lag model based on the result of the Lagrange Multiplier test. The per capita income and the proportion of people older than 65 years of age are still significantly and negatively associated with the T_{mrt} after controlling the spatial autocorrelation effects. The proportion of Hispanics and the proportion of people under 18 years old age have no significant association with the T_{mrt} .

4. Discussion

Extreme heat is an increasing threat to public health in cities. With the changing climate, more and more cities are exposed to more frequent extreme heatwaves. While a lot of attention has been paid on the urban-rural temperature gradients, the heat intensity also varies from neighborhood to neighborhood within the city. Understanding the fine level spatial distribution of the human heat stress level would be helpful for developing strategies to minimize the negative impacts of extreme heat in cities and building more equitable and resilient cities in terms of thermal comfort. This study firstly conducted a large-scale human outdoor heat exposure modeling at the city level and mapped the distribution of the averaged mean radiant temperature (T_{mrt}) in hot summer using urban microclimate modeling based on fine level digital city models and hourly meteorological data. Different from the widely used remote sensing-based land surface temperature, the T_{mrt} is more reasonable to represent human body energy balance and indicate human outdoor heat exposure in the summer with consideration of the air temperature, spatial-temporal distribution of shade, terrestrial radiation, humidity, and wind speed.

4.1. The spatial distribution of outdoor heat exposure

The results show that the outdoor heat exposure distributes unevenly across Philadelphia. Generally, the eastern and the southern parts of Philadelphia are experiencing higher-level outdoor heat exposure in the summer compared with the northwestern and the northeastern parts. The T_{mrt} is highly associated with the tree canopy cover and those areas with more tree canopies tend to have lower T_{mrt} . In addition, the high-rise buildings would also cast shadow on the ground and make the T_{mrt} lower. The eastern and southern parts of Philadelphia, which are featured by dense low-rise buildings patterned as concrete checkerboard and low vegetation canopies are suffering more from the outdoor heat exposure than the northwestern and northeastern regions where have large tree canopy covers.

The correlation analysis results show that the tree canopy cover is significantly and negatively correlated with the T_{mrt} , which indicates that increasing the tree canopy cover would reduce the outdoor heat exposure. Similar to previous studies that the T_{mrt} is significantly affected by the geometries of urban canyons (Herrmann & Matzarakis, 2012; Lau, Lindberg, Rayner, & Thorsson, 2015; Martinelli & Matzarakis, 2017; Rodríguez-Algeciras et al., 2018), correlation analysis results show that the height of the building is negatively correlated with the T_{mrt} , which indicates that the high-rise buildings would provide shade and help to reduce the T_{mrt} . The percentage of impervious surface is positively correlated with higher T_{mrt} . These results are similar to previous studies using overhead view satellite imagery methods to monitor the ground surface temperature (Chen et al., 2006; Equere et al., 2020). This is because tree canopies would help to provide shade and reduce the direct sunlight exposure to pedestrians, while the non-building impervious surface cannot block the sunlight from reaching the ground. The tree canopy height and the percentage of tree canopy cover have a stronger negative correlation with the T_{mrt} than the average building height, which means that the vegetation canopy would play a more important role in reducing the potential human heat exposure. Increasing the tree canopy and reducing the impervious surface would

be good strategies to mitigate outdoor heat exposure in hot summers. However, from 2008 to 2018 the tree canopy cover in Philadelphia has decreased by 6% (Philadelphia Tree Canopy Assessment, 2018), which brings more challenges to the extreme heat mitigation in Philadelphia. The current tree canopy cover in Philadelphia is 20 % and there is still a lot of space across the city for trees planting, especially in those neighborhoods of northern and southern regions. The spatial distribution of the outdoor heat exposure in this study would provide new insight for future urban tree planting projects in Philadelphia to reduce the resident's heat stress, especially for those neighborhoods with a higher level of outdoor heat exposure.

4.2. Environmental inequities in terms of heat exposure

A precise understanding of who is more vulnerable to extreme heat is important for developing strategies to adapt to extreme heat (Gronlund, 2014). This study investigated the outdoor heat exposure level in different neighborhoods of the study area. Different from the previously reported thermal inequities in other major US cities (Dialesandro, Brazil, Wheeler, & Abunnasr, 2021; Mitchell & Chakraborty, 2015), statistical analysis results show that there is no significant disparity in terms of outdoor heat exposure among different racial/ethnic groups in Philadelphia. The economic status and age groups are significantly associated with outdoor heat exposure. Similar to previous studies (Chakraborty, Hsu, Manya, & Sheriff, 2019; Mitchell & Chakraborty, 2015), the high-income people tend to live in neighborhoods with low outdoor heat exposure. This is because the rich people tend to pay more to live in more affluent neighborhoods with larger tree canopy covers or high-rise commercial areas, where the outdoor heat exposure level is lower. In Philadelphia, the elderly live in neighborhoods with low outdoor heat exposure. Since the old people are more sensitive and vulnerable to extreme heat (Åström, Bertil, & Joacim, 2011; Kovats & Koppe, 2005), living in cooler neighborhoods would be beneficial for their health. In addition, the elderly can have more outdoor activities in a more thermally comfortable environment during summer, which would reduce the chronic disease caused by physical inactivity.

4.3. Limitations and future work

There are still several limitations that need to be improved in future studies. Firstly, because of the computational intensity and the data availability, this study only uses the meteorological data of one year from June 1st to August 31st in 2018 to represent the overall outdoor heat exposure level in the study area. Future studies should use a longer time range in order to better represent the outdoor heat exposure level more objectively. In addition, future studies should also predict future heat exposure distributions in order to better evaluate the potential threat from heat events. Since more pixel operations in the urban microclimate modeling are parallelizable, future studies should explore using parallel computing to accelerate the urban microclimate modeling.

In addition, this study only models the dynamic of the environment while human mobilities are not considered. In order to better indicate human actual outdoor heat exposure, future studies should also consider the human mobilities and movements, and travel modes, etc. This study only used the mean radiant temperature, which indicates the thermal conditions of the environment. Future studies should use more human-centric metrics to indicate more personal human thermal comfort such as, physiologically equivalent temperature (PET), universal thermal climate index (UTCI), etc. Since different people have different sensitivity to heat exposure levels, therefore, future work should incorporate more personal characteristics, such as age, gender in order to better indicate personal heat exposure information.

Finally, this study only considers the outdoor heat exposure in the daytime, which cannot fully indicate human indoor heat stress and human heat stress at night. Future studies should also examine the

indoor heat stress level and nighttime heat stress.

5. Conclusion

This study estimated and investigated the spatial distribution of human outdoor heat exposure levels across neighborhoods of Philadelphia using urban microclimate modeling based on fine-level urban geometry derived from LiDAR data and meteorological data. This study generated a very fine level human outdoor heat exposure map in Philadelphia based on a more human-centric method – mean radiant temperature (T_{mrt}) to indicate the human thermal comfort. Generally, the northwestern part, northwestern part, and the downtown area of Philadelphia have lower heat exposure level than the southern and eastern parts. The tree canopy is the major factor that impacts human outdoor heat exposure. The vegetation canopy coverage, canopy height, and building height all provide shade and help to reduce the potential outdoor heat exposure in the city, while the impervious surface is associated with increasing outdoor heat exposure. Statistical results show that there is no significant disparity in terms of outdoor heat exposure across racial/ethnic groups in Philadelphia. Generally, the elderly people, who are more vulnerable to extreme heat, live in neighborhoods with lower heat exposure in summer. The higher-income people tend to live in more thermally comfortable neighborhoods.

Declaration of Competing Interest

The authors report no declarations of interest.

Acknowledgement

This work is partly supported by Microsoft AI for Earth Grant.

References

- Alexander, L. V., & Arblaster, J. M. (2009). Assessing trends in observed and modelled climate extremes over Australia in relation to future projections. *International Journal of Climatology*, 29(3), 417–435.
- Ali-Toudert, F., & Mayer, H. (2007). Effects of asymmetry, galleries, overhanging facades and vegetation on thermal comfort in urban street canyons. *Solar Energy*, 81(6), 742–754.
- Arnberger, A., Allex, B., Eder, R., Ebenberger, M., Wanka, A., Kolland, F., ... Hutter, H. P. (2017). Elderly resident's uses of and preferences for urban green spaces during heat periods. *Urban Forestry & Urban Greening*, 21, 102–115.
- Åström, D. O., Bertil, F., & Joacim, R. (2011). Heat wave impact on morbidity and mortality in the elderly population: A review of recent studies. *Maturitas*, 69(2), 99–105.
- Borden, K. A., & Cutter, S. L. (2008). Spatial patterns of natural hazards mortality in the United States. *International Journal of Health Geographics*, 7(1), 1–13.
- Bruse, M. (2004). ENVI-met 3.0: Updated model overview. Retrieved from: University of Bochum www.envi-met.com.
- CDC, Center for Disease Control. (2004). About extreme heat. Available at <http://www.bt.cdc.gov/disasters/extremeheat/about.asp>.
- Chakraborty, T., Hsu, A., Manya, D., & Sheriff, G. (2019). Disproportionately higher exposure to urban heat in lower-income neighborhoods: A multi-city perspective. *Environmental Research Letters*, 14(10), Article 105003.
- Chen, X. L., Zhao, H. M., Li, P. X., & Yin, Z. Y. (2006). Remote sensing image-based analysis of the relationship between urban heat island and land use/cover changes. *Remote Sensing of Environment*, 104(2), 133–146.
- Chen, L., Yu, B., Yang, F., & Mayer, H. (2016). Intra-urban differences of mean radiant temperature in different urban settings in Shanghai and implications for heat stress under heat waves: A GIS-based approach. *Energy and Buildings*, 130, 829–842.
- Dialesandro, J., Brazil, N., Wheeler, S., & Abunnasr, Y. (2021). Dimensions of thermal inequity: Neighborhood social demographics and urban heat in the Southwestern US. *International Journal of Environmental Research and Public Health*, 18(3), 941.
- Doick, K. J., Peace, A., & Hutchings, T. R. (2014). The role of one large greenspace in mitigating London's nocturnal urban heat island. *The Science of the Total Environment*, 493, 662–671.
- Easterling, D. R., Meehl, G. A., Parmesan, C., Changnon, S. A., Karl, T. R., & Mearns, L. O. (2000). Climate extremes: Observations, modeling, and impacts. *Science*, 289, 2068–2074.
- Eqere, V., Mirzaei, P. A., & Riffat, S. (2020). Definition of a new morphological parameter to improve prediction of urban heat island. *Sustainable Cities and Society*, 56, Article 102021.
- Frohlich, D., Gangwisch, M., & Matzarakis, A. (2019). Effect of radiation and wind on thermal comfort in urban environments—Application of the RayMan and SkyHelios model. *Urban Climate*, 27, 1–7.
- Gabriel, K. M. A., & Endlicher, W. R. (2011). Urban and rural mortality rates during heat waves in Berlin and Brandenburg, Germany. *Environmental Pollution*, 159(8–9), 2044–2050.
- Gál, C. V., & Kántor, N. (2020). Modeling mean radiant temperature in outdoor spaces, A comparative numerical simulation and validation study. *Urban Climate*, 32, Article 100571.
- Gronlund, C. J. (2014). Racial and socioeconomic disparities in heat-related health effects and their mechanisms: A review. *Current Epidemiology Reports*, 1(3), 165–173.
- Guo, A., Yang, J., Xiao, X., Xia, J., Jin, C., & Li, X. (2020). Influences of urban spatial form on urban heat island effects at the community level in China. *Sustainable Cities and Society*, 53, Article 101972.
- Harlan, S. L., Brazel, A. J., Prashad, L., Stefanov, W. L., & Larsen, L. (2006). Neighborhood microclimates and vulnerability to heat stress. *Social Science & Medicine*, 63(11), 2847–2863.
- Herrmann, J., & Matzarakis, A. (2012). Mean radiant temperature in idealised urban canyons—Examples from Freiburg, Germany. *International Journal of Biometeorology*, 56(1), 199–203.
- Hsu, A., Sheriff, G., Chakraborty, T., & Manya, D. (2021). Disproportionate exposure to urban heat island intensity across major US cities. *Nature Communications*, 12(1), 2721. <https://doi.org/10.1038/s41467-021-22799-5>
- Huang, G., Zhou, W., & Cadenasso, M. L. (2011). Is everyone hot in the city? Spatial pattern of land surface temperatures, land cover and neighborhood socioeconomic characteristics in Baltimore, MD. *Journal of Environmental Management*, 92(7), 1753–1759.
- Huang, J., Cedeno-Laurent, J. G., & Spengler, J. D. (2014). CityComfort+: A simulation-based method for predicting mean radiant temperature in dense urban areas. *Building and Environment*, 80, 84–95.
- Huttnner, S. (2012). *Further development and application of the 3D microclimate simulation ENVI-met*. Doctoral dissertation, Universitätsbibliothek Mainz.
- Johnson, D. P., Stanforth, A., Lulla, V., & Luber, G. (2012). Developing an applied extreme heat vulnerability index utilizing socioeconomic and environmental data. *Applied Geography*, 35(1–2), 23–31.
- Kim, Y., & Chun, Y. (2019). Revisiting environmental inequity in Southern California: Does environmental risk increase in ethnically homogeneous or mixed communities? *Urban Studies*, 56(9), 1748–1767.
- Klemm, W., Heusinkveld, B. G., Lenzholzer, S., & van Hove, B. (2015). Street greenery and its physical and psychological impact on thermal comfort. *Landscape and Urban Planning*, 138, 87–98.
- Kong, F., Yin, H., James, P., Hutyra, L. R., & He, H. S. (2014). Effects of spatial pattern of greenspace on urban cooling in a large metropolitan area of eastern China. *Landscape and Urban Planning*, 128, 35–47.
- Kovats, R. S., & Koppe, C. (2005). *Heatwaves: Past and future impacts on health. Integration of public health with adaptation to climate change: Lessons learned and new directions* (pp. 136–160).
- Landry, S. M., & Chakraborty, J. (2009). Street trees and equity: Evaluating the spatial distribution of an urban amenity. *Environment and Planning A*, 41(11), 2651–2670.
- Lau, K. K. L., Ren, C., Ho, J., & Ng, E. (2016). Numerical modelling of mean radiant temperature in high-density sub-tropical urban environment. *Energy and Buildings*, 114, 80–86.
- Lau, K. K. L., Lindberg, F., Rayner, D., & Thorsson, S. (2015). The effect of urban geometry on mean radiant temperature under future climate change: A study of three European cities. *International Journal of Biometeorology*, 59(7), 799–814.
- Li, X., Zhang, C., Li, W., & Kuzovkina, Y. A. (2016). Environmental inequities in terms of different types of urban greenery in Hartford, Connecticut. *Urban Forestry & Urban Greening*.
- Lin, J., Wang, Q., & Li, X. (2021). Socioeconomic and spatial inequalities of street tree abundance, species diversity, and size structure in New York City. *Landscape and Urban Planning*, 206, Article 103992.
- Lindberg, F., & Grimmond, C. S. B. (2011). The influence of vegetation and building morphology on shadow patterns and mean radiant temperature in urban areas: Model development and evaluation. *Theoretical and Applied Climatology*, 105(3), 311–323.
- Lindberg, F., Holmer, B., & Thorsson, S. (2008). SOLWEIG 1.0—Modelling spatial variations of 3D radiant fluxes and mean radiant temperature in complex urban settings. *International Journal of Biometeorology*, 52(7), 697–713.
- Lindberg, F., Grimmond, C. S. B., Gabey, A., Huang, B., Kent, C. W., Sun, T., ... Zhang, Z. (2018). Urban Multi-scale Environmental Predictor (UMEP): An integrated tool for city-based climate services. *Environmental Modelling & Software*, 99, 70–87.
- Lindberg, F., Onomura, S., & Grimmond, C. S. B. (2016). Influence of ground surface characteristics on the mean radiant temperature in urban areas. *International Journal of Biometeorology*, 60(9), 1439–1452.
- Martinelli, L., & Matzarakis, A. (2017). Influence of height/width proportions on the thermal comfort of courtyard typology for Italian climate zones. *Sustainable Cities and Society*, 29, 97–106.
- Matzarakis, A., Rutz, F., & Mayer, H. (2007). Modelling radiation fluxes in simple and complex environments—Application of the RayMan model. *International Journal of Biometeorology*, 51(4), 323–334.
- Matzarakis, A., Rutz, F., & Mayer, H. (2010). Modelling radiation fluxes in simple and complex environments: Basics of the RayMan model. *International Journal of Biometeorology*, 54(2), 131–139.
- Mayer, H., & Höpke, P. (1987). Thermal comfort of man in different urban environments. *Theoretical and Applied Climatology*, 38(1), 43–49.
- McDonald, R. I., Biswas, T., Sachar, C., Housman, I., Boucher, T. M., Balk, D., ... Leyk, S. (2021). The tree cover and temperature disparity in US urbanized areas: Quantifying the association with income across 5,723 communities. *PloS One*, 16(4), Article e0249715.

- McGeehin, M. A., & Mirabelli, M. (2001). The potential impacts of climate variability and change on temperature-related morbidity and mortality in the United States. *Environmental Health Perspectives*, 109(suppl 2), 185–189.
- McPhearson, T., Mustafa, A., & Ortiz, L. (2020). Heat and coronavirus can be twin killers. *Nature*, 582(7810), 32–32.
- Medina-Ramón, M., Zanobetti, A., Cavanagh, D. P., & Schwartz, J. (2006). Extreme temperatures and mortality: Assessing effect modification by personal characteristics and specific cause of death in a multi-city case-only analysis. *Environmental Health Perspectives*, 114(9), 1331–1336.
- Mitchell, B. C., & Chakraborty, J. (2015). Landscapes of thermal inequity: Disproportionate exposure to urban heat in the three largest US cities. *Environmental Research Letters*, 10(11), Article 115005.
- Mitchell, B. C., & Chakraborty, J. (2018). Exploring the relationship between residential segregation and thermal inequity in 20 US cities. *Local Environment*, 23(8), 796–813.
- Norton, B. A., Coutts, A. M., Livesley, S. J., Harris, R. J., Hunter, A. M., & Williams, N. S. (2015). Planning for cooler cities: A framework to prioritise green infrastructure to mitigate high temperatures in urban landscapes. *Landscape and Urban Planning*, 134, 127–138.
- Patz, J. A., Campbell-Lendrum, Holloway, T., & Foley, J. A. (2005). Impact of regional climate change on human health. *Nature*, 438, 310–317.
- Philadelphia Tree Canopy Assessment. (2018). *Philadelphia tree canopy assessment*. <http://treephilly.org/wp-content/uploads/2019/12/Tree-Canopy-Assessment-Report-Philadelphia-2018.pdf>.
- Reid, C. E., O'neill, M. S., Gronlund, C. J., Brines, S. J., Brown, D. G., Diez-Roux, A. V., & Schwartz, J. (2009). Mapping community determinants of heat vulnerability. *Environmental Health Perspectives*, 117(11), 1730–1736.
- Reid, C. E., Mann, J. K., Alfasso, R., English, P. B., King, G. C., Lincoln, R. A., ... Woods, B. (2012). Evaluation of a heat vulnerability index on abnormally hot days: An environmental public health tracking study. *Environmental Health Perspectives*, 120 (5), 715–720.
- Rodríguez-Algeciras, J., Tablada, A., Chaos-Yeras, M., De la Paz, G., & Matzarakis, A. (2018). Influence of aspect ratio and orientation on large courtyard thermal conditions in the historical centre of Camagüey-Cuba. *Renewable Energy*, 125, 840–856.
- Schwartz, J. (2005). Who is sensitive to extremes of temperature? A case-only analysis. *Epidemiology*, 16(1), 67–72.
- Shandas, V., Voelkel, J., Williams, J., & Hoffman, J. (2019). Integrating satellite and ground measurements for predicting locations of extreme urban heat. *Climate*, 7(1), 5.
- Stone, B., Hess, J. J., & Frumkin, H. (2010). Urban form and extreme heat events: Are sprawling cities more vulnerable to climate change than compact cities? *Environmental Health Perspectives*, 118(10), 1425–1428.
- Thorsson, S., Lindberg, F., Björklund, J., Holmer, B., & Rayner, D. (2011). Potential changes in outdoor thermal comfort conditions in Gothenburg, Sweden due to climate change: The influence of urban geometry. *International Journal of Climatology*, 31(2), 324–335.
- Thorsson, S., Rocklöv, J., Konarska, J., Lindberg, F., Holmer, B., Dousset, B., & Rayner, D. (2014). Mean radiant temperature—A predictor of heat related mortality. *Urban Climate*, 10, 332–345.
- Yang, J., Jin, S., Xiao, X., Jin, C., Xia, J. C., Li, X., & Wang, S. (2019). Local climate zone ventilation and urban land surface temperatures: Towards a performance-based and wind-sensitive planning proposal in megacities. *Sustainable Cities and Society*, 47, Article 101487.